ADVANCED MATERIALS

DOI: 10.1002/adma.200502199

Electric-Field-Controlled Surface Instabilities in Soft Elastic Films**

By *Narasimhan Arun*, *Ashutosh Sharma*, *Vijay B. Shenoy*, and *K. S. Narayan**

Understanding morphological instabilities at soft interfaces is important in a variety of diverse problems, such as adhesion/debonding in polymer films[1] and biological cells,[2] friction,[3] cavitation, and patterning.[4] Non-specific interactions of electromagnetic origin play an important role in these instabilities. Spontaneous surface patterns appear in soft solid films that are in contact proximity (< 50 nm) with a rigid contactor (or another film) due to a competition between destabilizing van der Waals attractive force (between the film and the contactor) and the stabilizing elastic-strain energy. It is known that the wavelength of the pattern that appears depends only on the film thickness.[5–7] These instabilities, while profoundly influencing the adhesion/debonding characteristics,[8] also provide an attractive route to patterning and morphological control of soft thin films by external interactions. However, intermolecular interactions, being material properties, cannot be easily modulated. Moreover, these interactions are short-ranged and thus even nanometer-scale surface roughness and defects affect the robustness of these patterns.

Here, we show the effect of electric fields on the generation and movement of patterns on solid surfaces. Previously, external fields have been used only to control surface instabilities and patterns in thin liquid films[9–15] where, unlike the solid films, the instability is dominated by a long-wavelength mode and is strongly dependent on the field strength and its decay characteristics. Unlike the control of liquid movement[16] and wetting/dewetting[17] by electric fields, the movement, adhesion/debonding, and pattern formation in soft solids by electric-field-induced elastic deformations are completely unexplored phenomena. The application of an electric field modulates the morphology, dimensionality, and the adhesive strength of surface patterns—elements that are useful in the design of smart adhesives. On application of an electric field, distinct morphological changes to the patterns are observed. These are "edge straightening", "finger elongation", and "pillar formation". This ability of the electric field to control these adhesive and morphological properties of a soft interface can also be employed to engineer surface structures for microfluidics[18] and soft-lithography[19,20] related applications.

Our experimental setup consisted of a wedge-shaped geometry schematically shown in Figure 1. A contactor is placed on top of a soft elastic film with one end on the film and the other on top of a spacer. The contact between the cover slip and the film engenders a zone of complete adhesive contact terminating in a finger pattern and an air gap (d) between the cover slip and the film ahead of the finger patterns. The air gap in this wedge geometry increases along the y-direction away from the contact zone. The finger patterns cease to exist in the absence of the top contactor. Small-amplitude, well-defined finger patterns (Fig. 2a), formed due to the adhesive van der Waals[6] interactions were ensured before turning on the voltage. Upon introduction of the voltage the patterns were modified. The response to the electric field (EF) can be classified based on the appearance of three distinct surface morphologies: "edge straightening" (Fig. 2b), "finger elongation" (Fig. 2c), and "pillar formation" (Fig. 2d). The manner in which the patterns evolve depended on the film parameters such as the shear modulus (μ) and the thickness (h). These emerging morphologies can be understood in terms of the stiffness parameter (μ/h) (the ratio of the shear modulus to that of the thickness of the elastic film). "Edge straightening", "finger elongation" and "pillar formation" processes were observed for high, intermediate, and low stiffness (μ/h) films, respectively.

For highly stiff films ($10\ \mu m < h < 100\ \mu m$ and $\mu > 6$ MPa), the electric field appreciably decreases the amplitude (a) of the initial finger patterns beyond a critical voltage (φ_{cric}). It is observed that the amplitude decrease is not accompanied by any discernable change in the wavelength of the finger pattern. The straightening of the finger pattern occurs asymmetrically, with a decreasing with respect to a stationary tip of the finger pattern, leading to complete intimate contact (Fig. 2b, inset). A complete straightening of the fingers happens, i.e., $a \to 0$, leading to a straight edge at a higher voltage (Fig. 2b). Further increase in the voltage results in a gradual displacement of this linear edge towards regions of lower electrostatic energy, thereby increasing the adhesive contact area. The other features that are observed are: i) φ_{cric} does not depend significantly on the ramping rate or on the polarity of the voltage. The emergent morphology is dependent on the electrostatic

[*] Prof. K. S. Narayan, N. Arun
Chemistry and Physics of Materials Unit
Jawaharlal Nehru Centre for Advanced Scientific Research
Bangalore 560064 (India)
E-mail: narayan@jncasr.ac.in
Prof. A. Sharma
Department of Chemical Engineering
Indian Institute of Technology
Kanpur 208016 (India)
Prof. V. B. Shenoy
Material Research Centre and Centre for Condensed Matter Theory
Indian Institute of Science
Bangalore 560012 (India)

[**] A. S. and V. B. S. acknowledge the support of DST, India, Nanoscience and Technology Program.

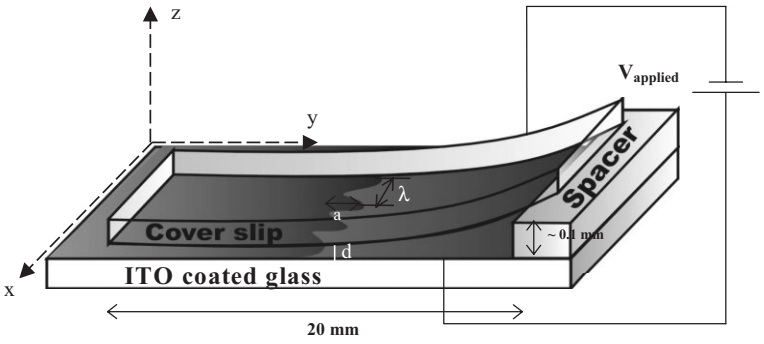

Figure 1. Schematic of the experiment. The left part of the cover slip (contactor) is in contact with the soft polydimethylsiloxane film on indium tin oxide (ITO) glass, while the right part is well above the film. Due to the presence of the spacer, the air gap d increases along the y-direction. The wavy pattern in the middle shows the "finger pattern" with wavelength λ. The area of the film in contact with the top cover slip is shaded. $V_{applied}$: applied voltage.

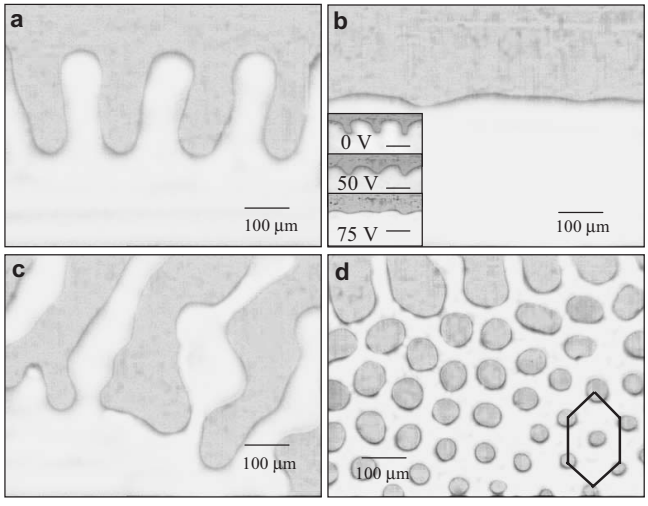

Figure 2. a) Typical finger pattern in absence of electric field (shear modulus $\mu = 3.9$ MPa and thickness $h = 37.2$ μm); b–d) "edge straightening" (high-stiffness parameter films, $\mu = 6.9$ MPa and $h = 76.8$ μm), "elongation" (intermediate stiffness parameter films, $\mu = 3.95$ MPa and $h = 37.2$ μm), and "pillar formation" (low stiffness parameter films, $\mu = 2.2$ MPa and $h = 29.9$ μm) under a suitable electric field, respectively. The inset in (b) shows the pattern-straightening process as a function of the applied voltage.

energy (square of voltage). ii) The "edge straightening" behavior is reversible as the initial small-amplitude fingers reappear on switching off the EF, but the recovery time is quite slow (as long as thirty minutes) compared to a nearly instantaneous response in the EF switch-on experiment. The slow recovery of the pattern is indicative of weak adhesive interactions in the absence of the electric force.

The response to the EF for films of intermediate stiffness parameter (4 MPa $< \mu <$ 6 MPa and 10 μm $< h <$ 100 μm) is different. Beyond a critical voltage (φ_{cric}), the amplitude of the finger pattern rapidly increases by an order of magnitude (~0.2 mm to 2 mm). These patterns continue to evolve beyond $\varphi > \varphi_{cric}$. The tips of the growing and expanding finger patterns ultimately undergo multiple scissions (tip splitting), leading to the formation of patterns with a network of undulating fingers (Fig. 2c). It is observed that this "elongation" process is irreversible; i.e., upon switching off the voltage, the patterns remain trapped in the new metastable state. The fingers remain elongated and do not relax back to the original configuration even after one day.

In the case of films with low stiffness (1 MPa $< \mu <$ 4 MPa and 10 μm $< h <$ 100 μm), an array of pillars of nearly circular cross section emerge above a critical value of the EF. Beyond φ_{cric}, the film surface ahead of the finger pattern (the region initially not in contact with the top contactor) spontaneously rises to form a row of pillars without any appreciable change in the finger pattern. It is interesting to note that the spacing between the pillars in the x-direction along a row is also proportional to the wavelength of the adjacent finger pattern. Upon further increase of voltage, the diameter of the circular pillars increases and additional rows of pillars emerge. The pillar diameter and its adhesive zone decreases as a function of distance in the y-direction from the original fingers. These features can be attributed to the weakening of the electric field with an increase in the distance due to the wedge geometry. The pillars are arranged in a nearly hexagonal periodic arrangement, with a spacing of ~3.5 h (Fig. 2d), consistent with the theoretical calculations of contact elastic instability.[21] The short-wave spacing of the solid pillars observed is independent of the magnitude of the local electric field, which is in complete contrast to the long-wave lateral structures observed in the case of liquid films where the periodic spacing is a strong function of the local electric field.[11] The periodic pillar pattern is sustained for a long period (~24 h), even after the removal of the field, highlighting the metastability of the field-induced pillars.

The critical voltage (φ_{cric}) to induce a morphological change in the initial finger pattern can be estimated analytically by the following energy-minimization procedure. The total energy of a film configuration consists of electrostatic capacitive energy that favors morphological change and elastic-strain energy that exerts a stabilizing influence. Due to the curved geometry of the contactor (cover slip), the air gap d separating the contactor from the film surface gradually varies along the y-direction (see Fig. 1), while the gap distance is constant along the x-direction. The important region of interest is the zone just ahead of the finger patterns where new patterns appear and d (< 100 nm) $\ll h$. This allows for an approximate quasi-one-dimensional stability analysis in the y-direction. The total potential energy density (energy per unit length) at a particular d is

$$\Pi(u) = \frac{1}{L}\int_0^L \left(-\frac{1}{2}\frac{\varepsilon_p \varepsilon_0 \varphi^2}{(\varepsilon_p d + h) - (\varepsilon_p - 1)u(x)}\right)dx + \frac{\mu}{2h}\sum_n a_n^2 S(hk_n) \quad (1)$$

where u is the normal (periodic) elastic displacement of the film surface, ε_p is the dielectric constant of the film, ε_0 is the

ADVANCED MATERIALS

permittivity of space, a_n are the Fourier amplitudes of the displacement (for the associated wavenumber $k_n = 2\pi n/L$, where L is the length of the film). In Equation 1, the function

$$S(\xi) = \frac{2\xi(1 + \cosh(2\xi) + 2\xi^2)}{\sinh(2\xi) - 2\xi} \quad (2)$$

is the dimensionless elastic stiffness of the Fourier mode with wavenumber k_n.[21] Taking $u = a_n \exp(i k_n x)$, the energy density (Eq. 1) for the mode k_n accurate to second order in a_n is

$$\Pi = \left(\frac{\mu}{2h} S(hk_n) - \frac{1}{2}\frac{(\varepsilon_p - 1)^2 \varepsilon_p \varepsilon_0 \varphi^2}{(\varepsilon_p d + h)^3}\right) a_n^2 \quad (3)$$

For voltages greater than φ_{cric}, the term in the parenthesis of the above equation becomes negative, signifying a lowering of the energy by deformation. The most unstable mode corresponds to the lowest elastic stiffness S, which gives $h k_n = 2.12$ or wavelength $\lambda \sim 3$ h, which is indeed seen to be the case for all the structures reported here. The critical voltage can then be obtained as

$$\varphi_{cric}^2 = \frac{6.22\mu}{h}\frac{(\varepsilon_p d + h)^3}{(\varepsilon_p - 1)^2 \varepsilon_p \varepsilon_0} \quad (4)$$

For a polydimethylsiloxane (PDMS) film ($\varepsilon_{PDMS} \sim 3$, $\mu \sim 1$ MPa) of thickness 10 μm and a gap distance 0.1 μm ($d \ll h$), the calculated critical voltage of ~2500 V is within an order of magnitude of the experimental observations of 200–500 V for similar films. The lower values seen in experiments are due to the compliance (bending) of the elastic contactor, which is not incorporated in the simple stability analysis. Furthermore, roughness and inhomogeneities on the film surface contribute to enhancement of local electric fields leading to lower critical voltages. The electric-field-induced morphological evolution occurs at much larger gap distances than the case of short-ranged van der Waals forces (critical gap distance < 5 nm).[7] Another important outcome of the analysis is that the wavelength of the emerging pattern depends linearly on the film thickness and not on the applied voltage (so long as it is above the critical voltage).

Figure 3 depicts the variation of φ_{cric} with the film parameters for the onset of morphological changes corresponding to "edge straightening", "finger elongation" and "pillar formation". The variations indicate that φ_{cric} depends linearly on h, with a weaker dependence on μ of the films. In the zone where patterns form $d \ll h$, the above equation gives $\varphi_{cric} \propto h\sqrt{\frac{E}{\mu}}$. Thus, φ_{cric} depends linearly on the film thickness, as is indeed observed in the experiments (Fig. 3). The linear dependence of φ_{cric} with thickness h is independent of the precise morphology and is only weakly sensitive to shear modulus. However, the shear modulus governs the morphology.

A morphological phase diagram as shown in Figure 4, in terms of the variable external parameters μ and h, summarizes the entire set of observations. The diagram also reveals the crossover pathways across the phase boundaries. For example, at a constant thickness $h \sim 40$ μm, as μ is increased from 3 MPa to 7 MPa, the surface-morphology pattern accordingly changes from the "pillar formation" to the "finger elongation" phase, and finally to the "edge straightening" phase.

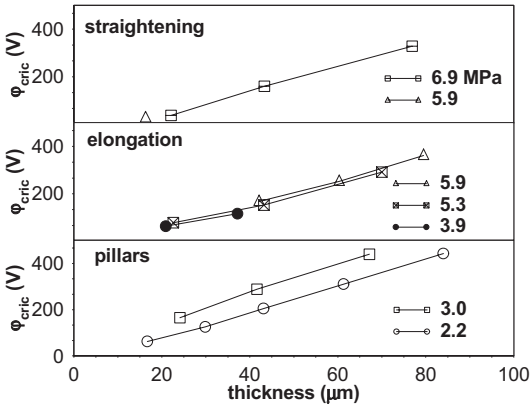

Figure 3. Critical voltage φ_{cric} versus thickness h of PDMS films with different μ for each morphological phase.

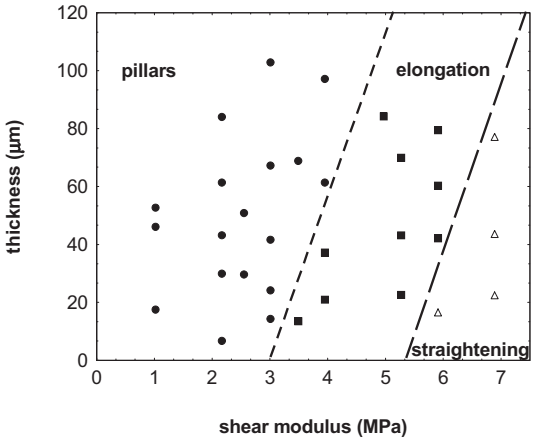

Figure 4. The phase diagram (μ versus h) obtained from EF-induced patterns in PDMS films. The dashed lines are a guide to the eye and represents the phase boundary.

The emergent morphology of the film subsequent to the attainment of criticality depends strongly on different competing energies in the system: the elastic deformation energy of the film, the bending energy of the flexible contactor, and the electrostatic capacitive energy. As the voltage is increased, the electrostatic energy essentially favors a larger area of contact between the cover slip and the film surface. This increase of contact area may be achieved differently in two limits. If the bending energy of the contactor is small compared to the elastic-deformation energy of the film, then the contactor can deform substantially to form complete contact, but the film deformation is minimized due to the high elastic-energy penalty. Both of these factors encourage formation of a zone of uniform contact and inhibit pattern formation. Since the elastic deformation energy is controlled by the stiffness parameter μ/h, these conditions are achieved where the film has high shear modulus and small thickness. Indeed, the "edge straightening" phase occurs in the region of the phase diagram where the shear modulus is large and thickness is small (Fig. 4). In the second limit,

where the elastic-deformation energy of the film is very small compared to the bending energy of the contactor, the increase of contact area is achieved by spontaneous surface deformation of the film without changing the configuration (curvature) of the contactor so that its bending energy is not significantly increased. Thus, films of relatively small stiffness parameter, vis-à-vis stiffness of the contactor, form pillar patterns as indeed seen in the morphology diagram shown in Figure 4.

In the intermediate case of a comparable energy cost for the deformation of the film and the contactor, finger elongation occurs by "bending" of the contactor in the direction parallel to the fingers so that the gap distance is reduced and fingers propagate by bridging the gap. The stiffness parameter of the film in this case is larger than in the case of pillar formation, but lower than that of the straightening case. This promotes large-amplitude fingering patterns with higher contact area and thus a higher electrostatic (adhesive) energy gain, with a lower elastic energy penalty as compared to the case of the pillar-like patterns. These trends are evident in recent computer simulations performed to understand these features and will be discussed elsewhere.

Finally, the reason "elongated fingers" or "pillars" once formed do not regain the original configuration after removal of the electric field is due to "adhesion–debonding" hysteresis.[8] As shown previously,[8] an energy functional which includes short-ranged van der Waals interactions contains many local minima (metastable states). This is because once contact is established, short-range attractive intermolecular interactions (such as the van der Waals component of adhesive energy) are sufficient to maintain adhesion. The elastic restoring forces for films with relatively smaller stiffness parameters are not strong enough to restore the original configuration (prior to the application of the electric field). Thus, the patterned state produced by application of electric field is a deep metastable minimum for films of lower stiffness parameters. The same metastable configuration is also responsible for the well-known persistence of the patterns[8] during separation of the contactor to distances greater than where the instability first appears (adhesion–debonding hysteresis) in a pure contact experiment (without electric field). On the other hand, for films with high stiffness parameters (Fig. 4), the straightened configuration of the contact meniscus is the energy minimum only in the presence of the applied electric field. Thus, upon its removal, the original small-amplitude finger pattern is recovered since the elastic restoring forces are strong owing to the high stiffness parameter. The viscoelasticity influences only the dynamics of the partial recovery. Furthermore, it is observed experimentally that the film maintains its integrity, i.e., it does not undergo plastic deformation or fracture.

In summary, we have shown that an electric field can control the adhesion, morphology, and movement of soft solid surfaces. Zones of unbroken intimate contact, hexagonally arranged pillars, and large-amplitude fingers are produced under different film stiffness and thickness conditions, and can be explained by the physics of electric-field-induced contact instabilities. This approach can be utilized to address issues related to adhesion and debonding. The possibility to obtain strikingly different surface patterns and structures, controlled by the material parameters, can lead to interesting applications such as on-demand mesostructures and offers a relatively simple route for large-area, rapid surface modifications. These results may have technological implications related to smart adhesives and mesopatterning. The unique feature in the "pillar formation" and "finger elongation" cases is the pattern formation on cured polymer film surfaces even in the absence of pre-patterned electrodes.

Experimental

Thin films of PDMS (Sylgard 184) were coated on pre-cleaned, transparent, conducting ITO substrates. The thickness (10 μm $< h <$ 120 μm) and the shear modulus (1 MPa $< \mu <$ 7 MPa) of these films were changed by varying the speed of the spin-coater and the crosslinker concentration, respectively. Films were then annealed at 60 °C for 4 h to obtain the crosslinked elastic films. A flexible contactor (Dow Corning cover glass, 2.2 cm × 2.2 cm, thickness ~225 μm) was then placed on the elastic film so that one end of the contactor was in contact with the film whereas the other end was supported on top of a 100 μm thick spacer (as shown schematically in Fig. 1). The flexible contactor was coated with gold (thickness ~50 nm). Experiments were carried out with the gold-coated side of the contactor on top and the other (non-coated) side in contact with the film to avoid arcing and shorting between the electrodes. The correction due to the presence of the additional intermediate glass-dielectric layer is accounted for in the data. The effective voltage (φ) in the contact zone is $\sim V_{\text{applied}}/[1 + \{(\varepsilon_g/\varepsilon_p)(h_g/h_p)\}]$ (where V_{applied} is the applied voltage, ε_g and ε_p are relative dielectric constants of glass and PDMS, respectively, and h_g and h_p are the thicknesses of glass and PDMS, respectively).

Received: October 13, 2005
Final version: December 15, 2005
Published online: February 6, 2006

[1] A. J. Crosby, *J. Mater. Sci.* **2003**, *38*, 4439.
[2] D. A. Hammer, M. Tirrell, *Annu. Rev. Mater. Sci.* **1996**, *26*, 651.
[3] M. Tirrell, *Langmuir* **1996**, *12*, 4548.
[4] A. M. Higgins, R. A. L. Jones, *Nature* **2000**, *404*, 476.
[5] A. Ghatak, M. K. Chaudhury, V. B. Shenoy, A. Sharma, *Phys. Rev. Lett.* **2000**, *85*, 4329.
[6] A. Ghatak, M. K. Chaudhury, *Langmuir* **2003**, *19*, 2621.
[7] V. B. Shenoy, A. Sharma, *Phys. Rev. Lett.* **2001**, *86*, 119.
[8] J. Sarkar, V. B. Shenoy, A. Sharma, *Phys. Rev. Lett.* **2004**, *93*, 018 302.
[9] D. G. Bucknall, *Prog. Mater. Sci.* **2004**, *49*, 713.
[10] E. Schaffer, T. Thurn-Albrecht, T. P. Russell, U. Steiner, *Nature* **2000**, *403*, 874.
[11] E. Schaffer, T. Thurn-Albrecht, T. P. Russell, U. Steiner, *Europhys. Lett.* **2001**, *53*, 518.
[12] M. D. Morariu, N. E. Voicu, E. Schaffer, Z. Lin, T. P. Russell, U. Steiner, *Nat. Mater.* **2003**, *2*, 48.
[13] D. Salac, W. Lu, C.-W. Wang, A. M. Sastry, *Appl. Phys. Lett.* **2004**, *85*, 1161.
[14] A. Oron, S. H. Davis, S. G. Bankoff, *Rev. Mod. Phys.* **1997**, *69*, 931.
[15] Y. S. Kim, H. H. Lee, *Adv. Mater.* **2003**, *15*, 332.
[16] R. A. Hayes, B. J. Feenstra, *Nature* **2003**, *425*, 383.
[17] Z. Lin, T. Kerle, T. P. Russell, E. Schaffer, U. Steiner, *Macromolecules* **2002**, *35*, 6255.
[18] S. K. Sia, G. M. Whitesides, *Electrophoresis* **2003**, *24*, 3563.
[19] Y. Xia, G. M. Whitesides, *Annu. Rev. Mater. Sci.* **1998**, *28*, 153.
[20] M. Geissler, Y. Xia, *Adv. Mater.* **2004**, *16*, 1249.
[21] J. Sarkar, A. Sharma, V. B. Shenoy, *Langmuir* **2005**, *21*, 1457.